ACS Catalysis

Research Article

pubs.acs.org/acscatalysis

Synergistic Promotion of Co/SiO_2 Fischer–Tropsch Catalysts by Niobia and Platinum

Jan H. den Otter, Sebastiaan R. Nijveld,[†] and Krijn P. de Jong*

Department of Inorganic Chemistry and Catalysis, Debye Institute for Nanomaterials Science, Utrecht University, Universiteitsweg 99, NL-3584 CG Utrecht, The Netherlands

Supporting Information

ABSTRACT: Transition-metal oxides and noble metals are well-known selectivity and activity promoters in cobalt-based Fischer–Tropsch catalysis. Niobia has been shown as an effective selectivity promoter as support material; however, its low porosity limits the cobalt loading. To combine the selectivity-promoting properties of niobia with a highly porous support, niobia-modified silica was prepared and applied as a support for Co and PtCo catalysts with cobalt loadings up to 21 wt %. Niobia promotion was found to increase the C_{5+} selectivity at 1 bar; however, it appeared to be ineffective at 20 bar. Promotion of Co/SiO_2 by a combination of platinum and niobia yielded an increase of the cobalt-weight normalized activity by a factor of 2–3 in the case of amorphous niobia and by a factor of 3–4 with niobia nanocrystals present, due to both an increased number of active sites and an increased cobalt-surface specific activity (turnover frequency).

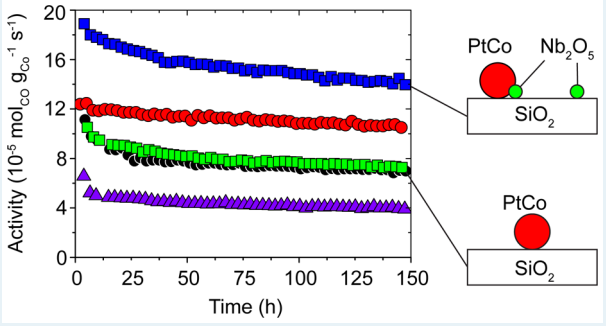

KEYWORDS: *Fischer–Tropsch, niobia, activity promotion, selectivity promotion, noble metal, transition-metal oxide*

INTRODUCTION

Synthesis gas, a mixture of H_2 and CO, can be obtained from feedstocks other than crude oil, such as natural gas, coal, and biomass. Via the Fischer–Tropsch process synthesis gas can be catalytically converted into ultraclean transportation fuels and chemicals. The Fischer–Tropsch reaction is typically catalyzed by iron or cobalt catalysts. Utilization of iron catalysts leads to the formation of (lower) olefins, the building blocks for a range of products such as polymers, solvents, and drugs.[1] Cobalt catalysts exhibit higher selectivity toward high-molecular-weight, paraffinic waxes which can be hydrocracked to produce lubricants and diesel fuels.[2−7]

The active phase, i.e. metallic cobalt, is usually supported by mesoporous metal oxides, which provide thermal, mechanical, and chemical stability. High support pore volume and surface area allow for facile catalyst preparation and mass transfer and high cobalt dispersion, respectively. The nature of the support, typically SiO_2, Al_2O_3, or TiO_2, determines the interaction with cobalt species. Strongly interacting supports such as γ-Al_2O_3 usually lead to high cobalt oxide dispersions but also hard to reduce cobalt species and vice versa.[8,9] Cobalt oxide reduction was found to be difficult, especially for small particles or in the case of strong interaction with the support[10] and can be promoted by the addition of a noble metal such as Pt, Pd, Ru, or Re. The role of the noble metal is to catalyze the reduction of cobalt oxide by H_2, leading to a higher degree of reduction at lower temperature and ultimately a higher number of metallic cobalt surface sites.[3,11−13]

The desired Fischer–Tropsch products are most often heavy hydrocarbons, typically paraffinic waxes, which can be hydrocracked to isoalkanes in the diesel range. The desired product is usually indicated as C_{5+}, while the undesired product is methane. The selectivity is influenced by process conditions such as temperature,[14,15] pressure, and CO conversion[16] and by catalyst properties such as support acidity,[17,18] pore diameter,[17,19] and transition-metal oxide (TMO) promotion.[5,20−26] Partially reducible TMO promoters such as manganese oxide, zirconia, titania, and niobia are typically added to promote the selectivity and activity of the catalyst by electronic interaction between cobalt and the TMO.[5,21−26] These TMO promoters can be present as small particles in close vicinity to or on the cobalt particles or as support material.[26] In the latter case decoration of cobalt particles by partially reduced TMO species might still occur due to strong metal–support interaction (SMSI) as reported by Tauster et al. and Haller et al.[27−29]

For cobalt catalysts supported by niobia, high selectivities toward heavy hydrocarbons have been reported.[14,30−34] The selectivity-promoting effect of niobia as support material was attributed to partial reduction of the support and formation of Co^0-NbO_x species due to SMSI as in the case of TiO_2, where TiO_x suboxides were observed.[35−40] For niobia-supported catalysts cobalt-weight normalized activities were reported similar to those for γ-Al_2O_3-supported catalysts. Upon noble-

Received: October 27, 2015
Revised: December 29, 2015
Published: January 22, 2016

DOI: 10.1021/acscatal.5b02418
ACS Catal. 2016, 6, 1616−1623

metal promotion, a factor of 2−3 increase of the cobalt-weight normalized activity has been reported for catalysts supported by partially reducible oxides such as TiO_2 and Nb_2O_5, which could not be explained by the number of active sites based on H_2 chemisorption.[2,41−43] This indicates that the intrinsic activity of the active sites increased, which is rare in cobalt Fischer−Tropsch catalysts. Iglesia et al. proposed that the activity-promoting role of Ru in Co/TiO_2 was related to inhibited deactivation by carbon.[41]

Typically, partially reducible oxides have a low specific surface area and porosity in comparison to SiO_2 and γ-Al_2O_3 and consequently the cobalt loading is limited (<10 wt %). For niobia-supported catalysts, low catalyst-weight normalized activities are obtained in comparison to catalysts with high cobalt loadings of 20−25 wt %. In this study niobia-modified silica is proposed as support to combine the selectivity-promoting electronic properties of niobia and a high-surface-area matrix to arrive at high activities.

Preparation of niobia-modified SiO_2, Al_2O_3, TiO_2, MgO, and ZrO_2 was reported before using impregnation, chemical vapor deposition, and sol−gel routes and various niobium precursors such as niobium ethoxide, niobium pentachloride, niobium oxalate, and ammonium niobium oxalate. The support surface area remained intact upon niobium deposition, and after high-temperature calcination, retardation of support surface area loss was observed.[44,45] At low loading niobium was found to be present in isolated NbO_4 sites; at higher loading polymerization occurred to NbO_6 sites and ultimately Nb_2O_5 nanocrystals were formed.[46,47]

Niobia-modified Al_2O_3 (5−30 wt %) as support for cobalt Fischer−Tropsch catalysts was reported by Mendes et al.[37,38,48] and was prepared using an ammonium niobium oxalate complex. Niobia was found to form a multilayered structure, and the degree of polymerization increased with loading. At low niobia loading and catalysis at 1 bar, high methane and low C_{5+} selectivities were observed in comparison to an Al_2O_3-supported catalyst, attributed to the formation of Co^{2+}−Co^0 species, responsible for methanation. At high niobia loading after reduction at 500 °C lower methane and higher C_{5+} selectivity but reduced activity were observed, attributed to the formation of Co^0-NbO_x species, responsible for methyl radical formation and promotion of chain growth.

In this paper the extent and origin of activity and selectivity promotion by niobia and platinum on Co/SiO_2 Fischer−Tropsch catalysts[49,50] is investigated. Niobia-modified silica is prepared and investigated as support material for cobalt and platinum−cobalt Fischer−Tropsch catalysts with industrially relevant cobalt loadings up to ∼21 wt %. Catalyst performance is investigated at 1 bar and low CO conversion and under industrially relevant conditions, 20 bar and 30−40% CO conversion, and correlated to the catalyst structure.

EXPERIMENTAL SECTION

Preparation. Niobia-modified silica supports were prepared by incipient wetness impregnation[51] of a silica gel (Davisil 643, Sigma-Aldrich, >99%; SA_{BET}, 260 $m^2\ g^{-1}$; PV, 1.1 mL g^{-1}; PD, 17 nm) with an aqueous 70−200 g L^{-1} (0.22−0.66 M) ammonium niobium oxalate (ANO, Companhia Brasileira de Metalurgia e Mineração) solution. After it was dried overnight at 60 °C in stagnant air, the niobium precursor was calcined in a 0.5 L min^{-1} g_{sample}^{-1} air flow at 550−900 °C (2 h, 5 °C min^{-1}). Niobia-modified silica samples with niobia loading Nb/Si = 0−0.12 at./at. were prepared in multiple impregnation cycles and will be referred to as *X*NbSi-*Y*, where X is the atomic ratio Nb/Si and Y is the calcination temperature. An overview of the prepared supports can be found in Table S1 in the Supporting Information.

Cobalt was deposited on niobia-modified silica by impregnation[51] with an aqueous 4.0 M $Co(NO_3)_2$ solution or by coimpregnation with an aqueous 4.0 M $Co(NO_3)_2$, 0.03 M $Pt(NH_3)_4(NO_3)_2$ (Co/Pt = 140) solution, aiming for a cobalt loading of 0.9 $mg_{Co}\ m^{-2}$, corresponding to 9−21 wt % Co. After it was dried overnight at 60 °C in stagnant air, the cobalt nitrate precursor was calcined at 350 °C (2 h, 3 °C min^{-1}) in a 1 L min^{-1} g_{sample}^{-1} N_2 flow. Cobalt loading is expressed as the mass of metallic cobalt per gram of reduced catalyst. An overview of the prepared catalysts can be found in Table 1.

Characterization. Powder X-ray diffraction (XRD) patterns were measured using a Bruker-AXS D2 Phaser X-ray diffractometer using Co Kα radiation (λ = 1.789 Å). Nb_2O_5 crystallite size was calculated by applying the Scherrer equation (k = 0.9) to the (180) diffraction at 33° 2θ; Co_3O_4 crystallite size was calculated using the (311) diffraction at 43° 2θ.

N_2 physisorption measurements were performed at −196 °C, using a Micromeritics TriStar 3000 apparatus. Prior to analysis, ∼100 mg of the sample was dried at 200 °C for 20 h under an N_2 flow. The surface area was calculated using the BET theory for p/p_0 = 0.06−0.25. Pore diameter distribution was determined using the BJH theory applied to the adsorption branch. The pore volume was calculated from single-point adsorption at p/p_0 = 0.98.

Backscattered electron-scanning electron microscopy (BSE-SEM) images were acquired with an FEI Phenom type 1 SEM operated at 5 keV.

TEM samples were reduced in a 1 L min^{-1} g_{sample}^{-1} 25 vol % H_2/N_2 flow at 350 °C (2 h, 3 °C min^{-1}), exposed to air at room temperature, and subsequently embedded in a two-component epoxy resin (Epofix, EMS) and cured at 60 °C for at least 16 h. Using a Diatome Ultra 35° diamond knife mounted on a Reichert-Jung Ultracut E microtome, an embedded sample was cut in sections with a nominal thickness of 50 nm which were collected on a TEM grid. Bright field TEM and high angle annular dark field (HAADF) STEM imaging was performed on a Tecnai 20 microscope equipped with a field emission gun operated at 200 keV and EDX detector.

Temperature-programmed reduction (TPR) experiments were performed using a Micromeritics Autochem 2920 instrument. Typically 100 mg of the sample was dried at 120 °C for 1 h under an Ar flow and reduced up to 1000 °C (10 °C min^{-1}) in a 5 vol % H_2/Ar flow.

H_2 chemisorption measurements were performed using a Micromeritics ASAP 2020 instrument. Prior to the measurements, ∼200 mg of the sample was dried for 1 h under dynamic vacuum at 100 °C and reduced under an H_2 flow at 350 °C (1 °C min^{-1}, 2 h). H_2 adsorption isotherms were measured at 150 °C, as recommended by Reuel for supported cobalt particles.[52] Metallic cobalt-specific surface area and average particle size were calculated assuming the surface stoichiometry H/Co = 1 and an atomic cross-sectional area of 0.0662 nm^2.

Fischer−Tropsch Synthesis. Catalytic testing at 1 bar was performed using a U-shaped, continuous-flow, fixed-bed reactor system. Typically 10 mg of catalyst (38−75 μm) was diluted with 200 mg of SiC (200−400 μm) and loaded in a stainless steel reactor, i.d. = 3 mm, to achieve a bed height of 2 cm. A 500 mg portion of SiC was loaded on top of the catalyst bed to

DOI: 10.1021/acscatal.5b02418
ACS Catal. 2016, 6, 1616−1623

Table 1. Nb/Si Atomic Ratio, (Nb-)Si Calcination Temperature, (Nb-)Si Specific BET Surface Area, and Pt and Co Loadings Based on Intake and Assuming Nb To Be Present as Nb_2O_5 for (Pt)Co-(Nb)Si Catalysts

	support			catalyst	
catalyst designation	Nb/Si atomic ratio, at./at.	calcination temp, °C	specific surface area, $m^2\ g^{-1}$	Pt loading, wt %	Co loading,[a] wt %
Co-Si-550		550	269		21.0
Co-0.02NbSi-550	0.02	550	265		19.3
Co-0.04NbSi-550	0.04	550	262		18.8
Co-0.06NbSi-550	0.06	550	256		18.6
Co-0.09NbSi-550	0.09	550	250		19.8
Co-0.12NbSi-550	0.12	550	240		18.8
PtCo-Si-550		550	269	0.43	18.0
PtCo-0.02NbSi-550	0.02	550	265	0.46	19.1
PtCo-0.04NbSi-550	0.04	550	262	0.44	18.2
PtCo-0.06NbSi-550	0.06	550	256	0.43	17.8
PtCo-0.09NbSi-550	0.09	550	250	0.41	16.9
PtCo-0.12NbSi-550	0.12	550	240	0.40	16.6
Co-Si-900		900	115		9.2
Co-0.04NbSi-900	0.04	900	169		14.3
Co-0.12NbSi-900	0.12	900	155		11.6
PtCo-Si-900		900	115	0.21	8.6
PtCo-0.04NbSi-900	0.04	900	169	0.32	13.3
PtCo-0.12NbSi-900	0.12	900	155	0.28	11.8

[a]Corresponding to 0.8−1.0 $mg_{Co}\ m^{-2}$ for all catalysts; see Table S2 in the Supporting Information.

ensure gas preheating. The catalysts were reduced in situ at atmospheric pressure in a 33 vol % H_2/Ar flow, GHSV 180000 h^{-1}, at 350 °C (2 h, 5 °C min^{-1}). After the temperature was lowered to 220 °C, the gas stream was switched to synthesis gas: H_2/CO = 2.0 v/v, GHSV 18000−54000 h^{-1}, CO conversion 2−4%. Products up to C_{18} were analyzed using an online Varian 430-GC instrument equipped with FID. Activity and selectivity were calculated on the basis of the hydrocarbons formed. The reported catalyst performance was determined after at least 15 h on stream. Catalytic testing at 20 bar was performed using an Avantium Flowrence 16 parallel, continuous-flow, fixed-bed reactor system. A 30 mg portion of catalyst (38−75 μm) was diluted with 200 mg of SiC (200 μm) and loaded in a stainless steel reactor, i.d. = 2 mm, to achieve a bed height of 4−5 cm. The catalysts were reduced in situ at atmospheric pressure in a 25 vol % H_2/He flow, GHSV 6000−14000 h^{-1}, at 350 °C (8 h, 1 °C min^{-1}). After the temperature was lowered to 180 °C, the gas stream was switched to synthesis gas, H_2/CO = 2.0 v/v, GHSV 3000−8000 h^{-1}, and the reactors were pressurized to 20 bar and subsequently heated to 220 °C. The GHSV was adjusted to obtain 30−40% CO conversion. Products up to C_9 were analyzed using an online Agilent Technologies 7890A gas chromatograph. The reported catalyst performance was determined after at least 100 h on stream. The GHSV was defined as the total gas flow divided by the catalyst volume.

RESULTS AND DISCUSSION

Support Modification. Niobia-modified silica was prepared by (multiple) impregnations with an aqueous solution of ammonium niobium oxalate and subsequent drying and calcination at 550−900 °C. The Nb/Si atomic ratio was calculated to be 0−0.12. Assuming five Nb atoms per square nanometer, Nb/Si = 0.12 at./at. was calculated to correspond to a monolayer of niobia on silica.[45,53] An overview of all samples, including their designations, is shown in Table 1; niobia loadings (0−21 wt %) and porosity data are shown in Table S1 in the Supporting Information.

The silica porosity and pore diameter (~20 nm) was found to remain intact upon niobia modification (Figure S1 in the Supporting Information), as previously observed by Ko and Shiju.[54,55] The presence of niobia stabilized the SiO_2 structure during calcination at T > 550 °C, resulting in a less pronounced decrease of surface area and porosity than for SiO_2 calcined without niobia modification. After calcination at 550 °C, no niobia was observed using XRD, indicating strong interaction between niobia and silica. Calcination at higher temperatures led to niobia polymerization and formation of Nb_2O_5 crystallites (Figure 1). Niobia polymerization upon increased loading and calcination temperature was also inferred from

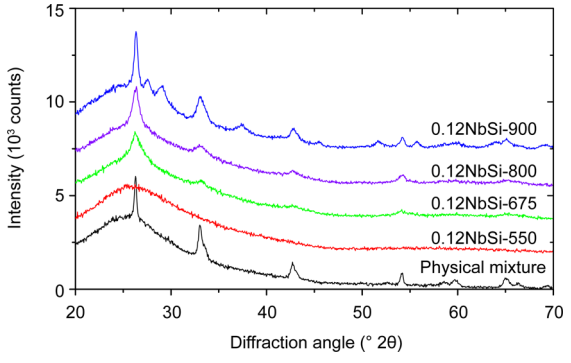

Figure 1. X-ray diffractograms (Co Kα radiation) for a physical mixture of ANO and SiO_2 (Nb/Si = 0.12 at./at.) after calcination at 550 °C and for 0.12NbSi-550, 0.12NbSi-675, 0.12NbSi-800, and 0.12NbSi-900. The dominant crystalline Nb_2O_5 phase was orthorhombic Nb_2O_5 (T-phase).

DOI: 10.1021/acscatal.5b02418
ACS Catal. 2016, 6, 1616−1623

diffuse reflectance spectroscopy results (Figure S2 in the Supporting Information).

Using TEM no niobia particles were observed after calcination at 550 °C (Figure 2, left). After calcination at 900 °C, crystalline 15−20 nm niobia particles were observed (dark dots in Figure 2, right). Using SEM, niobia was found to partially migrate to the exterior surface of the macroscopic grains (~50 μm) upon calcination at 900 °C (Figure S5 in the Supporting Information).

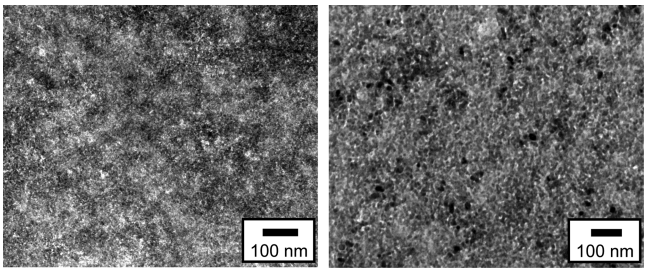

Figure 2. Bright field TEM images for (left) 0.12NbSi-550 and (right) 0.12NbSi-900. See Figure S3 in the Supporting Information for more images.

Niobia−Silica-Supported Cobalt Catalysts. An overview of the cobalt and platinum−cobalt catalysts prepared using niobia-modified silica as support is shown in Table 1.

After impregnation of niobia-modified silica with a cobalt precursor or coimpregnation with cobalt and platinum precursor and subsequent decomposition, the catalysts were studied using X-ray diffraction (Figure 3). Cobalt was found to be present as Co_3O_4, and from the XRD line broadening, the Co_3O_4 crystallite size was found to be 8−9 nm for Co-(Nb)Si-550 and 7−8 nm for PtCo-(Nb)Si-550, Co-(Nb)Si-900, and PtCo-(Nb)Si-900 (Table 2).

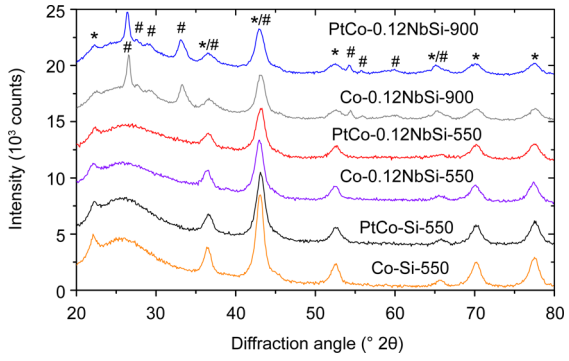

Figure 3. X-ray diffractograms (Co Kα radiation) for calcined (Pt)Co-(Nb)Si catalysts: (*) Co_3O_4 diffractions; (#) Nb_2O_5 diffractions.

Using TEM, the cobalt particle size was studied for reduced and passivated PtCo-NbSi catalysts after sample preparation using ultramicrotomy (Figure 4). The bright areas, which were well-distributed throughout the catalyst grain, were confirmed to be cobalt-rich; however, niobium oxide particles could not unambiguously be distinguished. On the basis of the analysis of 200−350 particles, the average cobalt particle sizes were calculated to be 5−9 nm (see Figure S6 in the Supporting Information).

For PtCo-0.12NbSi-900 a significantly smaller apparent cobalt oxide particle size, ~5 nm, was determined in comparison to that for the other samples. In this support crystalline niobia particles were observed using TEM and XRD, which would also appear as bright spots and could be confused with cobalt oxide particles, limiting the reliability of these measurements. For the other samples, the crystallite size obtained using XRD was similar to the particle size obtained in this TEM study. In Table 2 an overview is given of the cobalt particle sizes estimated on the basis of TEM.

Table 2. Co_3O_4 Crystallite Size Determined Using XRD and Calculated Co Crystallite Size, Metallic Cobalt-Specific Surface Area (MSA), and Apparent Co Particle Size (d_{app}) Determined using H_2 Chemisorption at 150 °C, and Co Particle Size Determined Using TEM for Co-Si, PtCo-Si, Co-NbSi and PtCo-NbSi Catalysts

	XRD		H_2 chemisorption		TEM
catalyst	Co_3O_4 (nm)	Co (nm)	MSA (m^2 g_{Co}^{-1})	Co d_{app} (nm)	Co (nm)
Co-Si-550	8.5	6.8	57	12	
Co-0.04NbSi-550	8.6	6.8	39	17	
Co-0.12NbSi-550	7.9	6.3	27	25	
PtCo-Si-550	7.6	6.0	95	7	
PtCo-0.04NbSi-550	7.1	5.7	76	9	8
PtCo-0.12NbSi-550	7.3	5.8	54	13	7[a]
Co-Si-900	6.8	5.4	50	14	
Co-0.04NbSi-900	7.2	5.7	46	15	
Co-0.12NbSi-900	7.6	6.0			6[a]
PtCo-Si-900	6.8	5.4	90	8	8[a]
PtCo-0.04NbSi-900	7.2	5.7	73	9	9
PtCo-0.12NbSi-900	7.0	5.6	73	9	5[a]

[a]Calculated from Co_3O_4 particle size using Co and Co_3O_4 densities; see Figure S6 in the Supporting Information.

The influence of niobia modification and Pt promotion on the cobalt oxide reduction behavior was studied using temperature-programmed reduction (TPR). Multiple reduction peaks were observed for the reduction of Co−Si (Figure 5). The peak at 300 °C is thought to be the reduction of Co_3O_4 to CoO, which usually is facile and quantitative.[8,39,56] Reduction peaks at higher temperatures were attributed to reduction of CoO to metallic Co. Due to strong interaction between CoO and silica and consequent formation of cobalt silicates, high reduction temperatures were required to obtain metallic cobalt.

Niobia modification did not have a large influence on the reducibility of Co−Si (Figure 5). The additional peak around 900 °C might be related to the formation of mixed Co−Nb oxides or Nb−Si oxides. Extensive overlap of reduction peaks of cobalt oxide, niobia, and probably mixed Co−Nb oxides impeded accurate quantitative determination of the degree of cobalt oxide reduction. No large influence of niobia modification (Figure 5) or support calcination temperature (Figure 5, right) on the reduction behavior was observed and the consequential effect of niobia modification on the degree of reduction was expected to be small on the basis of TPR data.

Pt promotion drastically reduced the temperature required for reduction of Co−Si (Figure 5), as observed before for noble-metal-promoted cobalt catalysts.[3,11,13] This will lead to a higher degree of cobalt oxide reduction for PtCo catalysts in comparison to Co catalysts after isothermal reduction at 350 °C. The small peak observed at 750 °C was attributed to reduction of cobalt silicates. For PtCo-0.12NbSi-550 (Figure 5,

DOI: 10.1021/acscatal.5b02418
ACS Catal. 2016, 6, 1616−1623

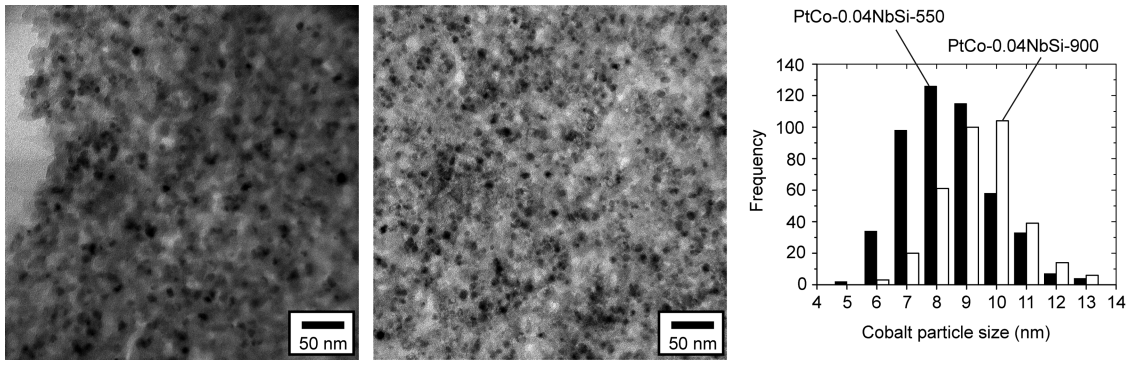

Figure 4. Bright field TEM images and cobalt particle size distribution for reduced and passivated PtCo-0.04NbSi-550 (left) and PtCo-0.04NbSi-900 (middle).

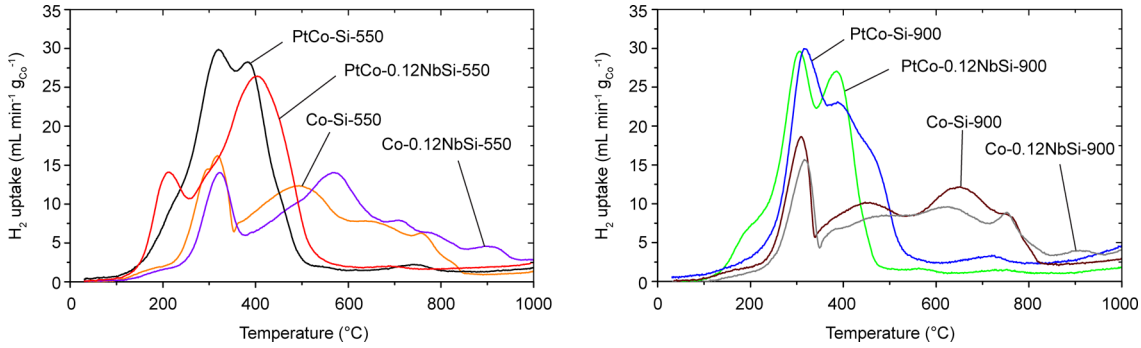

Figure 5. Temperature-programmed reduction profiles for (Pt)Co-(0.12Nb)Si-550 (left) and (Pt)Co-(0.12Nb)Si-900 (right).

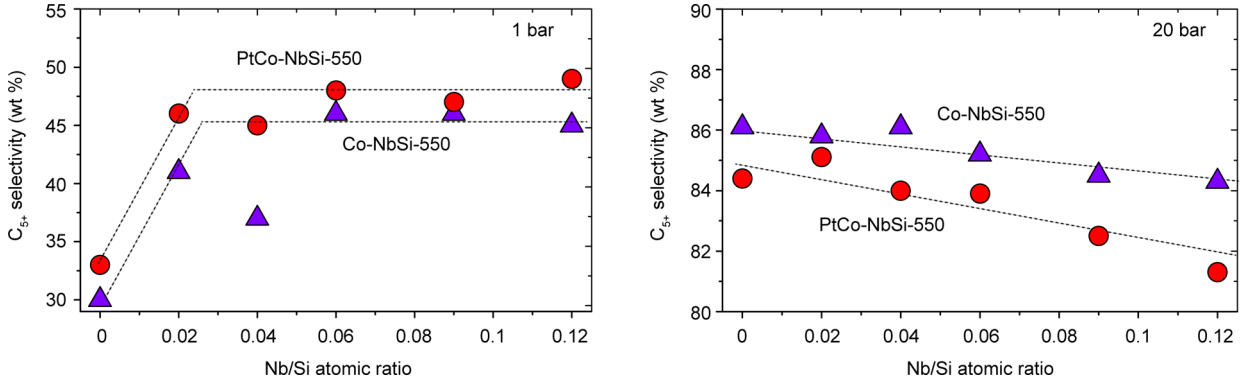

Figure 6. C_{5+} selectivity in Fischer−Tropsch synthesis at 220 °C and H_2/CO = 2.0 at 1 bar after 15 h on stream (left) and at 20 bar after 100 h on stream (right) for Co-NbSi-550 and PtCo-NbSi-550 catalysts. Lines are added to guide the eye.

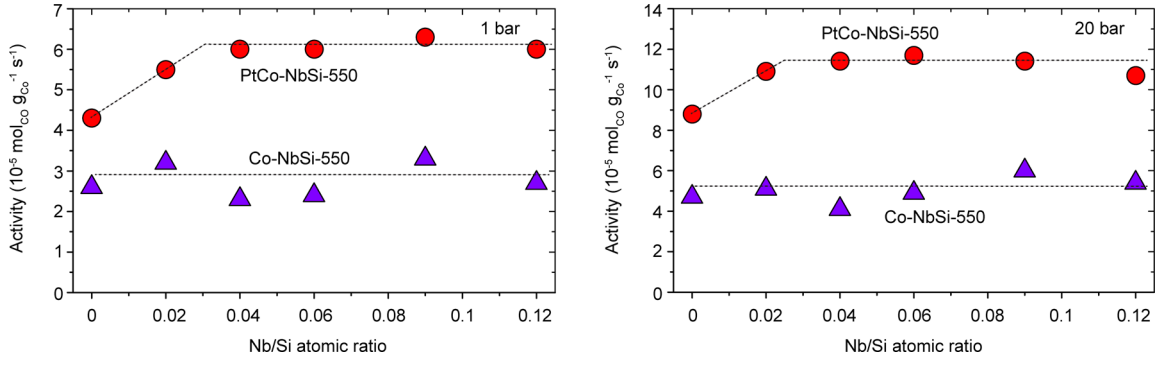

Figure 7. Cobalt-weight normalized Fischer−Tropsch activity at 220 °C and H_2/CO = 2.0 at 1 bar after 15 h on stream (left) and at 20 bar after 100 h on stream (right) for Co-NbSi-550 and PtCo-NbSi-550 catalysts. Lines are added to guide the eye.

DOI: 10.1021/acscatal.5b02418
ACS Catal. 2016, 6, 1616−1623

left) this peak was not observed, indicating that niobia modification of silica impeded the formation of cobalt silicates. The metallic cobalt-specific surface area (MSA) after catalyst reduction at 350 °C was measured using H_2 chemisorption at 150 °C (Table 2). The MSA was found to increase by a factor of 2 upon Pt promotion, most likely due to a higher degree of cobalt oxide reduction. Upon niobia modification, the MSA decreased for both Pt-promoted catalysts and non-Pt-promoted catalysts. This decreasing MSA was also observed by Johnson et al. upon Mn promotion of Co/SiO_2[24] and is attributed to coverage of the cobalt surface by niobia due to SMSI. This suppressed H_2 chemisorption was found to be less severe for catalysts prepared after support calcination at 900 °C, indicating that niobia was less reactive after high-temperature calcination. A potential method to overcome suppressed H_2 chemisorption due to SMSI would be by reduction and subsequent mild oxidation to remove niobia from the cobalt surface, followed by a second reduction cycle at lower temperature as proposed for TiO_2-supported catalysts,[58,59] and will be investigated in further studies on niobia-containing catalysts. Methods that could provide additional information on the number of sites participating in Fischer−Tropsch synthesis could be reversible CO chemisorption or sulfur poisoning; however, these were not investigated within the scope of this study.

Fischer−Tropsch Synthesis. The performance of (Pt-)Co/(Nb)Si was investigated in Fischer−Tropsch catalysis at 1 and 20 bar, 220 °C, and $H_2/CO = 2.0$. An overview of the C_{5+} selectivities is shown in Figure 6, and the cobalt-weight normalized activities are shown in Figure 7. Cobalt-weight normalized activity (CTY) at 20 bar during the first 150 h on stream is shown in Figure 8 for PtCo-Si and PtCo-NbSi

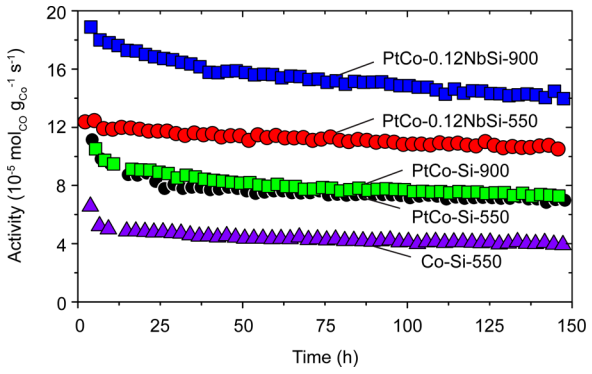

Figure 8. Cobalt-weight normalized Fischer−Tropsch activity at 20 bar, 220 °C, and $H_2/CO = 2.0$ for (Pt)Co-(Nb)Si catalysts.

catalysts. CH_4 and C_{5+} selectivities, CTY, and turnover frequencies at 20 bar are shown in Table 3; for data at 1 bar see Table S3 in the Supporting Information.

At 1 bar the C_{5+} selectivity of Co-Si and PtCo-Si was found to be around 30 wt % and increased to 45−50 wt % upon niobia modification (Figure 6, left). At 20 bar, the C_{5+} selectivity of Co-Si and PtCo-Si was 81−86 wt % and decreased slightly upon niobia modification (Figure 6, right). The influence of transition-metal oxide (TMO) promotion on the catalyst selectivity has been reported before to depend on the reactor pressure for MnO-promoted Co catalysts.[20,25,57] At elevated pressures no or only slight influence of TMO promotion on the catalyst selectivity was observed, which is thought to be related to the higher CO coverage at elevated pressure and consequent higher chain growth probability, even without the presence of a promoter, making TMO promotion for selectivity not mandatory.

Upon Pt promotion of Co-Si, the CTY was found to increase by a factor of 2 (Figure 7). No large effect of niobia modification on the CTY of Co-Si was observed. Promotion by a combination of platinum and niobia yielded a factor of 3 and 4 increase of the CTY in comparison to Co-Si for PtCo-NbSi-550 and PtCo-NbSi-900, respectively (Figure 8 and Table 3). The CTY of Co-(Nb)Si and PtCo-(Nb)Si was found to be a factor of 2 higher at 20 bar than at 1 bar. The influences of Pt promotion, niobia modification, and NbSi calcination temperature on the CTY were similar at 1 and at 20 bar.

Turnover frequencies (TOFs) were calculated on the basis of XRD, H_2-chemisorption, and TEM results (Table 3). The TOFs based on H_2 chemisorption results were calculated to be 0.033 and 0.037 s^{-1} for Co-Si-550 and PtCo-Si-550, respectively, which are similar to the TOFs reported previously for Co/SiO_2 and $PtCo/SiO_2$ catalysts.[49] This indicates that the observed increase of the CTY upon Pt promotion of Co-Si was largely caused by a higher number of active sites. This is in agreement with previous observations where noble-metal promotion of supported cobalt catalysts was reported to facilitate cobalt oxide reduction, leading to a higher degree of reduction, an increased number of active sites, and consequently higher CTY.[3,11,13]

The TOF calculated on the basis of XRD results was significantly lower than the TOF calculated on the basis of H_2 chemisorption results (Table 3). This was attributed to incomplete cobalt oxide reduction for Co-Si and Co-NbSi and suppressed H_2 chemisorption for Co-NbSi and PtCo-NbSi (vide supra). No large influence of niobia modification of Co-Si on the TOF based on Co_3O_4 crystallite size from XRD was observed (Table 3). On the basis of H_2 chemisorption results, the TOF was calculated to increase upon niobia modification; however, this is most likely related to an underestimated number of active sites due to SMSI, as also observed by Johnson et al.[24]

With a combination of niobia and platinum promotion both an increased number of active sites (Table 2) and an increased TOF (Table 3) in comparison to Co-Si were calculated on the basis of H_2 chemisorption, XRD, and TEM data. The calculated increase of CTY and TOF was more pronounced for PtCo-NbSi-900, in which niobia was present as 15−20 nm nanocrystals, than for PtCo-NbSi-550, where niobia was amorphous, indicating that the synergy between niobia nanocrystals and platinum more efficiently promoted the activity of Co-Si catalysts.

A turnover frequency increase was previously reported for noble-metal-promoted Co/TiO_2[2,41,43] and Co/Nb_2O_5[42] catalysts, both being a combination of noble-metal promotion and a partially reducible oxide support. In this study an increased TOF was also observed for catalysts promoted by niobia and for catalysts with high porosity and industrially relevant cobalt loadings.

A useful study that could provide additional insight in the role of Pt and niobia during the reaction rather than ex situ, for example the influence of reactants and products including H_2O under the reaction conditions, could be SSITKA; however, this was not investigated within the scope of this study.

DOI: 10.1021/acscatal.5b02418
ACS Catal. 2016, 6, 1616−1623

Table 3. Selectivity toward CH_4 and C_{5+}, CO Conversion (X_{CO}), Cobalt-Weight Normalized Activity (CTY), and Turnover Frequency (TOF) in Fischer−Tropsch Catalysis at 20 bar, 220 °C, and H_2/CO = 2.0 after 125 h on Stream for (Pt)Co-(Nb)Si Catalysts

	selectivity (wt %)				TOF (10^{-3} s^{-1})		
catalyst	CH_4	C_{5+}	X_{CO} (%)	CTY (10^{-5} mol_{CO} g_{Co}^{-1} s^{-1})	H_2	XRD	TEM
Co-Si-550	7	86	35	4.7	33	19	
Co-0.02NbSi-550	8	86	35	5.1		20	
Co-0.04 NbSi-550	7	86	28	4.1	42	17	
Co-0.06 NbSi-550	8	85	32	4.9		18	
Co-0.09 NbSi-550	9	85	29	6.0		24	
Co-0.12 NbSi-550	9	84	37	5.4	80	20	
PtCo-Si-550	8	84	39	8.8	37	31	
PtCo-0.02NbSi-550	8	85	39	11		41	
PtCo-0.04NbSi-550	8	84	36	11	60	38	57
PtCo-0.06NbSi-550	7	84	39	12		39	
PtCo-0.09NbSi-550	8	83	36	11		40	
PtCo-0.12NbSi-550	9	81	33	11	79	37	35
Co-Si-900	10	83	11	3.5	28	11	
Co-0.04 NbSi-900	9	81	29	5.6	49	19	
Co-0.12 NbSi-900	9	84	24	5.5		20	17
PtCo-Si-900	9	81	28	8.8	39	28	31
PtCo-0.04 NbSi-900	9	82	36	15	80	50	82
PtCo-0.12 NbSi-900	10	82	30	14	78	47	33

CONCLUSIONS

Niobia-modified silica (NbSi) with Nb/Si 0−0.12 at./at. was prepared by impregnation and subsequent calcination at 550−900 °C. At low loadings, Nb was present as small niobia particles or mixed Nb−Si species. Upon higher loadings and calcination temperatures a niobia layer was formed on SiO_2 and ultimately 15−20 nm nanocrystals were observed which partially migrated to the exterior surface of the silica grains. Co and PtCo catalysts with constant surface-specific loading of 0.8−1.0 mg_{Co} m^{-2} (9−21 wt % Co) were prepared by impregnation of the NbSi supports.

On the basis of XRD, H_2 chemisorption, and TEM data no evidence was found that niobia modification of silica had a large influence on the cobalt particle size of around 8 nm. Upon Pt promotion of Co-Si and Co-NbSi, cobalt oxide reduction was facilitated and the number of active sites was found to increase by a factor of 2.

At 1 bar the C_{5+} selectivity in Fischer−Tropsch catalysis increased significantly upon niobia modification, whereas at 20 bar it was found to only slightly decrease. This pressure dependence of niobia promotion is thought to be related to a higher intrinsic CO coverage at elevated pressures, making promotion with a transition-metal oxide for selectivity less effective at more elevated pressures.

The influences of Pt promotion, niobia modification, and NbSi calcination temperature on the catalyst activity were found to be identical at 1 bar and at 20 bar. Upon Pt promotion of Co/SiO_2, the cobalt-weight normalized activity was found to increase by a factor of 2 due to a higher number of active sites. Promotion of Co-Si by a combination of platinum and niobia yielded an increase of the cobalt-weight normalized activity by a factor of 2−3 in the case of amorphous niobia and a factor of 3−4 for niobia nanocrystals. This increase was partially attributed to an increased number of active sites and partially to an increased turnover frequency. The activity increase was highest for catalysts after NbSi calcination at 900 °C, indicating that synergistic promotion was more efficient between platinum and niobia nanocrystals than between platinum and amorphous or atomically dispersed niobia.

An increased turnover frequency was previously reported for noble-metal-promoted Co/Nb_2O_5 and Co/TiO_2, which both display quite low specific surface areas. In this study an increased TOF was obtained for supported Co catalysts promoted by niobia plus noble metal with high surface area and industrially relevant cobalt loadings.

ASSOCIATED CONTENT

Supporting Information

The Supporting Information is available free of charge on the ACS Publications website at DOI: 10.1021/acscatal.5b02418.

N_2 physisorption, diffuse reflectance spectroscopy, TEM and SEM data for (Nb)Si supports, and TEM data for (Pt)Co-(Nb-)Si catalysts (PDF)

AUTHOR INFORMATION

Corresponding Author

*E-mail for K.P.d.J.: K.P.deJong@uu.nl.

Funding

This research was financially supported by Companhia Brasileira de Metalurgia e Mineração-CBMM. Dr. Robson Monteiro and Mr. Rogério Ribas from CBMM are acknowledged for useful discussions and for supplying ANO samples. The authors thank Mr. Hans Meeldijk (ultramicrotomy and TEM), Ms. Nazila Masoud (ultramicrotomy), Mrs. Marjan Versluijs-Helder (XRD), Mr. Korneel Cats (TPR), Mr. Gang Wang (TPR), and Ms. Ilse van Ravenhorst (DRS) for assistance and execution of indicated analyses.

Notes

The authors declare no competing financial interest.

DOI: 10.1021/acscatal.5b02418
ACS Catal. 2016, 6, 1616−1623

[†]This author was a brilliant M.Sc. student who contributed greatly to this research; he passed away during the period of this study.

REFERENCES

(1) Torres Galvis, H. M.; Bitter, J. H.; Khare, C. B.; Ruitenbeek, M.; Dugulan, A. I.; de Jong, K. P. *Science* **2012**, *335*, 835−838.
(2) Iglesia, E. *Appl. Catal., A* **1997**, *161*, 59−78.
(3) Jacobs, G.; Das, T. K.; Zhang, Y.; Li, J.; Racoillet, G.; Davis, B. H. *Appl. Catal., A* **2002**, *233*, 263−281.
(4) *Studies in Surface Science and Catalysis*; Davis, B. H., Occelli, M. L., Eds.; Elsevier: Amsterdam, 2007; Vol. *163*, pp 1−420.
(5) Khodakov, A. Y.; Chu, W.; Fongarland, P. *Chem. Rev.* **2007**, *107*, 1692−744.
(6) Soled, S. L.; Iglesia, E.; Fiato, R. A.; Baumgartner, J. E.; Vroman, H.; Miseo, S. *Top. Catal.* **2003**, *26*, 101−109.
(7) Bezemer, G. L.; Bitter, J. H.; Kuipers, H. P. C. E.; Oosterbeek, H.; Holewijn, J. E.; Xu, X.; Kapteijn, F.; van Dillen, A. J.; de Jong, K. P. *J. Am. Chem. Soc.* **2006**, *128*, 3956−64.
(8) Jacobs, G.; Ji, Y.; Davis, B. H.; Cronauer, D.; Kropf, A. J.; Marshall, C. L. *Appl. Catal., A* **2007**, *333*, 177−191.
(9) Khodakov, A. Y. *Catal. Today* **2009**, *144*, 251−257.
(10) Khodakov, A. Y.; Lynch, J.; Bazin, D.; Rebours, B.; Zanier, N.; Moisson, B.; Chaumette, P. *J. Catal.* **1997**, *168*, 16−25.
(11) Diehl, F.; Khodakov, A. Y. *Oil Gas Sci. Technol.* **2009**, *64*, 11−24.
(12) Conner, W. C.; Falconer, J. L. *Chem. Rev.* **1995**, *95*, 759−788.
(13) Das, T. K.; Jacobs, G.; Patterson, P. M.; Conner, W. A.; Li, J.; Davis, B. H. *Fuel* **2003**, *82*, 805−815.
(14) Den Otter, J. H.; de Jong, K. P. *Top. Catal.* **2014**, *57*, 445−450.
(15) Van der Laan, G. P.; Beenackers, A. A. C. M. *Catal. Rev.: Sci. Eng.* **1999**, *41*, 255−318.
(16) Bukur, D. B.; Pan, Z.; Ma, W.; Jacobs, G.; Davis, B. H. *Catal. Lett.* **2012**, *142*, 1382−1387.
(17) Rane, S.; Borg, Ø.; Yang, J.; Rytter, E.; Holmen, A. *Appl. Catal., A* **2010**, *388*, 160−167.
(18) Rane, S.; Borg, Ø.; Rytter, E.; Holmen, A. *Appl. Catal., A* **2012**, *437*−*438*, 10−17.
(19) Borg, Ø.; Eri, S.; Blekkan, E. A.; Storsater, S.; Wigum, H.; Rytter, E.; Holmen, A. *J. Catal.* **2007**, *248*, 89−100.
(20) Bezemer, G. L.; Radstake, P. B.; Falke, U.; Oosterbeek, H.; Kuipers, H. P. C. E.; van Dillen, A.; de Jong, K. P. *J. Catal.* **2006**, *237*, 152−161.
(21) Morales, F.; de Smit, E.; de Groot, F. M. F.; Visser, T.; Weckhuysen, B. M. *J. Catal.* **2007**, *246*, 91−99.
(22) Morales, F.; de Groot, F. M. F.; Gijzeman, O.; Mens, A. J. M.; Stephan, O.; Weckhuysen, B. M. *J. Catal.* **2005**, *230*, 301−308.
(23) Moradi, G. R.; Basir, M. M.; Taeb, A.; Kiennemann, A. *Catal. Commun.* **2003**, *4*, 27−32.
(24) Johnson, G. R.; Werner, S.; Bell, A. T. *ACS Catal.* **2015**, *5*, 5888−5903.
(25) Dinse, A.; Aigner, M.; Ulbrich, M.; Johnson, G. R.; Bell, A. T. *J. Catal.* **2012**, *288*, 104−114.
(26) Prieto, G.; De Mello, M. I. S.; Concepción, P.; Murciano, R.; Pergher, S. B. C.; Martínez, A. *ACS Catal.* **2015**, *5*, 3323−3335.
(27) Tauster, S. J.; Fung, S. C. *J. Catal.* **1978**, *55*, 29−35.
(28) Tauster, S. J.; Fung, S. C.; Garten, R. L. *J. Am. Chem. Soc.* **1978**, *100*, 170−175.
(29) Haller, G. L.; Resasco, D. E. *Adv. Catal.* **1989**, *36*, 173−235.
(30) Frydman, A.; Soares, R. R.; Schmal, M. *Stud. Surf. Sci. Catal.* **1993**, *75*, 2797−2800.
(31) Silva, R. R. C. M.; Schmal, M.; Frety, R.; Dalmon, J. A. *J. Chem. Soc., Faraday Trans.* **1993**, *89*, 3975−3980.
(32) De Souza, C. D.; Cesar, D. V.; Marchetti, S. G.; Schmal, M. *Stud. Surf. Sci. Catal.* **2007**, *167*, 147−152.
(33) Soares, R. R.; Frydman, A.; Schmal, M. *Catal. Today* **1993**, *16*, 361−370.
(34) Dos Santos, A. C. B.; Pereira, A. T. ; Sousa-Aguiar, E. F.; Moraes, J. L.; de Oliveira, K. A.; Sugaya, M. D. F.; Schmal, M.; Monteiro, R. D. S.; Vicentini, V. P. Cobalt Catalyst for the Synthesis of Fischer−Tropsch, Catalyst Support, Processes for the Preparation of Support and Catalyst and the Use of the Catalyst. WO Patent 2005085390 A1, September 15, 2005.
(35) Ahón, V. R.; Lage, P. L. C.; de Souza, C. D.; Mendes, F. M. T.; Schmal, M. *J. Nat. Gas Chem.* **2006**, *15*, 307−312.
(36) Mendes, F. M. T.; Uhl, A.; Starr, D. E.; Guimond, S.; Schmal, M.; Kuhlenbeck, H.; Shaikhutdinov, S. K.; Freund, H.-J. *Catal. Lett.* **2006**, *111*, 35−41.
(37) Mendes, F. M. T.; Perez, C. a. C.; Noronha, F. B.; Schmal, M. *Catal. Today* **2005**, *101*, 45−50.
(38) Mendes, F. M. T.; Perez, C. A. C.; Noronha, F. B. *J. Phys. Chem. B* **2006**, *110*, 9155−9163.
(39) Noronha, F. B.; Perez, C. A.; Frety, R. *Phys. Chem. Chem. Phys.* **1999**, *1*, 2861−2867.
(40) Li, Y.; Fan, Y.; Yang, H.; Xu, B.; Feng, L.; Yang, M.; Chen, Y. *Chem. Phys. Lett.* **2003**, *372*, 160−165.
(41) Iglesia, E.; Soled, S. L.; Fiato, R. A.; Via, G. H. *J. Catal.* **1993**, *143*, 345−368.
(42) Noronha, F. B.; Frydman, A.; Aranda, D. A. G. A. G.; Perez, C.; Soares, R. R.; Morawek, B.; Castner, D.; Campbell, C. T. T.; Frety, R.; Schmal, M. *Catal. Today* **1996**, *28*, 147−157.
(43) Eschemann, T. O.; Oenema, J.; de Jong, K. P. *Catal. Today* **2016**, *261*, 60−66.
(44) Jehng, J.-M.; Wachs, I. E. *Catal. Today* **1993**, *16*, 417−426.
(45) Jehng, J.-M.; Wachs, I. E. *J. Mol. Catal.* **1991**, *67*, 369−387.
(46) Wachs, I. E. *Catal. Today* **1996**, *27*, 437−455.
(47) Wachs, I. E.; Briand, L. E.; Jehng, J.-M.; Burcham, L.; Gao, X. *Catal. Today* **2000**, *57*, 323−330.
(48) Mendes, F. M. T.; Perez, C. A.; Soares, R. R.; Noronha, F. B.; Schmal, M. *Catal. Today* **2003**, *78*, 449−458.
(49) Munnik, P.; de Jongh, P. E.; de Jong, K. P. *J. Am. Chem. Soc.* **2014**, *136*, 7333−40.
(50) Munnik, P.; Krans, N. A.; de Jongh, P. E.; de Jong, K. P. *ACS Catal.* **2014**, *4*, 3219−3226.
(51) Munnik, P.; de Jongh, P. E.; de Jong, K. P. *Chem. Rev.* **2015**, *115*, 6687−6718.
(52) Reuel, R. C. *J. Catal.* **1984**, *85*, 63−77.
(53) Prieto, G.; Concepción, P.; Martínez, A.; Mendoza, E. *J. Catal.* **2011**, *280*, 274−288.
(54) Ko, E. I.; Bafrali, R.; Nuhfer, N. T.; Wagner, N. J. *J. Catal.* **1985**, *95*, 260−270.
(55) Shiju, N. R.; Brown, D. R.; Wilson, K.; Rothenberg, G. *Top. Catal.* **2010**, *53*, 1217−1223.
(56) Sexton, B. *J. Catal.* **1986**, *97*, 390−406.
(57) Thiessen, J.; Rose, A.; Meyer, J.; Jess, A.; Curulla-Ferré, D. *Microporous Mesoporous Mater.* **2012**, *164*, 199−206.
(58) Soled, S. L.; Iglesia, E.; Fiato, R. A.; Baumgartner, J. E.; Vroman, H.; Miseo, S. *Top. Catal.* **2003**, *26*, 101−109.
(59) Tauster, S. *Acc. Chem. Res.* **1987**, *20*, 389−394.

DOI: 10.1021/acscatal.5b02418
ACS Catal. 2016, 6, 1616−1623